Nanoscale

Accepted Manuscript

This article can be cited before page numbers have been issued, to do this please use: H. Ye, D. Kitts, X. Wang, T. Wang, Y. Wang and T. Yang, *Nanoscale*, 2026, DOI: 10.1039/D6NR00796A.

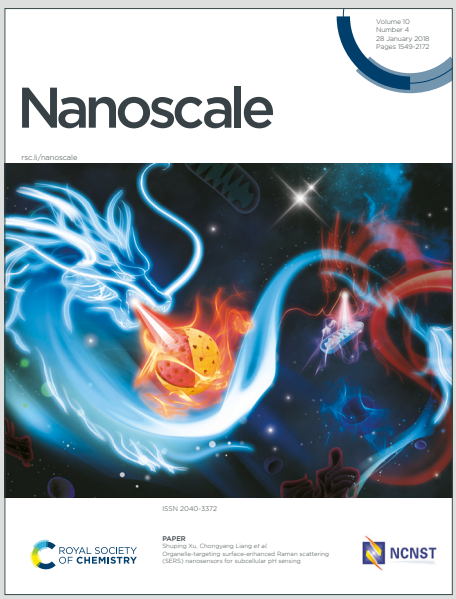

ROYAL SOCIETY OF CHEMISTRY

rsc.li/nanoscale

View Article Online
DOI: 10.1039/D6NR00796A

Tea Polyphenol Increases Nanoplastics Release from Plastic Cups but Mitigates Potential Detrimental Effects during Simulated Tea Drinking

*Haoxin Ye[a], David D. Kitts[a], Xiwen Wang[a], Tianyu Wang[a], Yifan Wang[a], and Tianxi Yang[a]**

a Food, Nutrition and Health, Faculty of Land and Food Systems, The University of British Columbia, Vancouver V6T1Z4, Canada

***Corresponding author: Tianxi Yang (tianxi.yang@ubc.ca)**

View Article Online
DOI: 10.1039/D6NR00796A

ABSTRACT

The presence of micro- and nanoplastics (MNPs) in daily life raises increasing concerns about their potential health and environmental impacts. However, how food components influence MNP release from packaging materials and the resulting exposure risks remains poorly understood. Here, we investigated the effect of the primary tea polyphenol, epigallocatechin gallate (EGCG), on MNPs release from polystyrene cups during a simulated tea-drinking process involving thermal treatments. A surface-enhanced Raman scattering sensor was developed to quantify released plastic particles *in situ* using EGCG-based luminescent metal–phenolic network labeling. The released particles were identified primarily as nanoplastics, and the presence of EGCG significantly ($P < 0.05$) increased MNPs release, particularly during microwave heating and most prominently upon repeated cup use. Interestingly, EGCG increased the MTT response of differentiated Caco-2 cells exposed to released NPs in a dose-dependent manner, suggesting a potential mitigation of NP-associated cytotoxicity under the tested in vitro conditions. This study provides new insight into the dynamic interactions between food components and plastic packaging during realistic consumption scenarios, revealing an overlooked pathway influencing human exposure to nanoplastics. The findings expand current understanding of contaminant release mechanisms at the food–environment interface and inform future strategies for exposure mitigation and sustainable material design to protect food safety, environmental and public health.

KEYWORDS: Nanoplastics exposure; food–environment interface; epigallocatechin gallate; luminescent metal–phenolic networks; SERS; food composition

View Article Online
DOI: 10.1039/D6NR00796A

INTRODUCTION

The practice of using plastics in many aspects of consumer daily activities, ranging from purchasing clothing and healthcare products to including a variety of packaged commodities used to increase shelf-life and food safety, is an ongoing practice in today's reality. The omnipresence of micro/nanoplastics (MNPs) has resulted in increased awareness of the consequences to ecological and environmental issues that relate to pollution of both land and sea habitats. It is estimated that 4.8 to 12.7 million tons of plastic enter the ocean annually; however, the magnitude of plastic emissions on land and into freshwater systems is significantly higher, thus posing an even greater environmental challenge.[1] A pressing concern is the transformation of conspicuous plastic waste derived from agricultural, food, and environmental systems into microplastics (MPs, with sizes ranging from 1 μm to 5 mm) and nanoplastics (NPs, smaller than 1 μm).[2] This process of release into the environment is facilitated by mechanical stress, photochemical, thermal, and biological decomposition; processes which fracture the plastic into smaller, more pervasive fragments.[3] These particles can readily disperse into ecosystems and water bodies, potentially on exposure, leading to a variety of human health issues that involve oxidative stress, cellular damage, inflammation, DNA damage, neurotoxic effects, and overall metabolic disturbances.[4,5]

Contemporary techniques for identifying and measuring MNPs typically utilize microscopic and spectroscopic approaches, such as Scanning Electron Microscopy (SEM) and Pyrolysis Mass Spectrometry (MS).[6–8] Despite the effectiveness of these procedures, significant challenges exist to increase the efficiency of establishing an accurate risk assessment. High costs, labor-intensive procedures, and the need for skilled operators are recognized hurdles required to overcome limitations for using rapid screening techniques.[9–11] Recent advances in rapid screening applications, such as smartphone-based fluorescence microscopy and handheld surface-enhanced Raman scattering (SERS) assays, can provide fast, on-the-spot, alternative methods of analysis. However, they, too, are hindered by a relatively lower sensitivity, thus reducing applicability in real-life situations.[12,13] Our prior research reported the development of an L-MPN-assisted SERS platform for the rapid and sensitive detection of plastic particles, which provides the basis for the EGCG-based adaptation used in the present study.[14] L-MPNs, a novel labeling strategy comprising of phenolic ligands, metal ions, and conventional dyes, was successful in facilitating a rapid (<5 minutes) labeling process for various plastic particles.[15] The robust Raman signals generated by the dyes used in our process allowed for serving as the Raman reporter, thereby enhancing sensitivity by up to 500 times, equivalent to an unprecedentedly low detection limit of 0.1 ppm for polystyrene (PS).[14] This innovative approach has significant promise for use to assess real-world plastic contamination scenarios.

View Article Online
DOI: 10.1039/D6NR00796A

Understanding the dynamics of exposure to MNPs in the food environment is a crucial step for mitigating potential risks to human health. Such exposures can occur through skin contact, inhalation, or ingestion, including seemingly benign activities such as drinking hot tea from plastic cups. Previous research has shown that the interaction of heat with plastic containers undeniably leads to the release of plastics into hot beverage fluids.[16] For example, plastic teabag studies demonstrated that brewing at 95 °C can release extremely large quantities of micro- and nanoplastics into tea, highlighting hot beverages as a realistic exposure route.[17] Although recent studies have shown that green tea extracts and catechin-rich systems can induce microplastic aggregation, reduce bioaccessibility, and suppress intestinal transport in vitro,[18] little is known about whether a specific tea polyphenol can influence the release of plastic particles from food-contact materials during beverage preparation or modify the subsequent biological response. Tea catechins, particularly epigallocatechin gallate (EGCG), are present in green tea or black tea and have well-known bioactive antioxidant and anti-inflammatory activities.[19,20] In addition to tea beverages, EGCG is also found in a range of different food products packaged in plastic containers, including dried fruits and nuts.[21,22] The relationship between EGCG and the release of plastic particles requires further investigation to understand potential implications for human health. Moreover, EGCG was selected in this study not to suggest a general performance advantage over other polyphenols (e.g., tannic acid), but because it uniquely serves a dual role in this food-relevant model system: as a representative tea polyphenol that may influence nanoplastics release and as a phenolic ligand capable of forming L-MPNs through coordination with metal ions and π-π interactions with dyes. By integrating an EGCG-based L-MPN labeling approach with our previously developed SERS platform, we achieved in situ monitoring of MNPs released from plastic cups within the same chemically relevant exposure scenario.

In this research, EGCG was selected not only for being a representative bioactive tea polyphenol [20], but also as a phenolic ligand candidate to form L-MPNs for SERS quantification of released plastic particles (Scheme 1). The novelty of this study is (i) applying an EGCG-based L-MPN labeling system to this specific PS cup model, (ii) revealing that EGCG can significantly influence nanoplastics release under simulated tea-drinking thermal conditions, and (iii) integrating release quantification with a preliminary biological-response assessment in differentiated Caco-2 cells. These results provide novel insights into contaminant release dynamics, exposure risk assessment, and the need for safer, more sustainable materials in food contact applications.

View Article Online
DOI: 10.1039/D6NR00796A

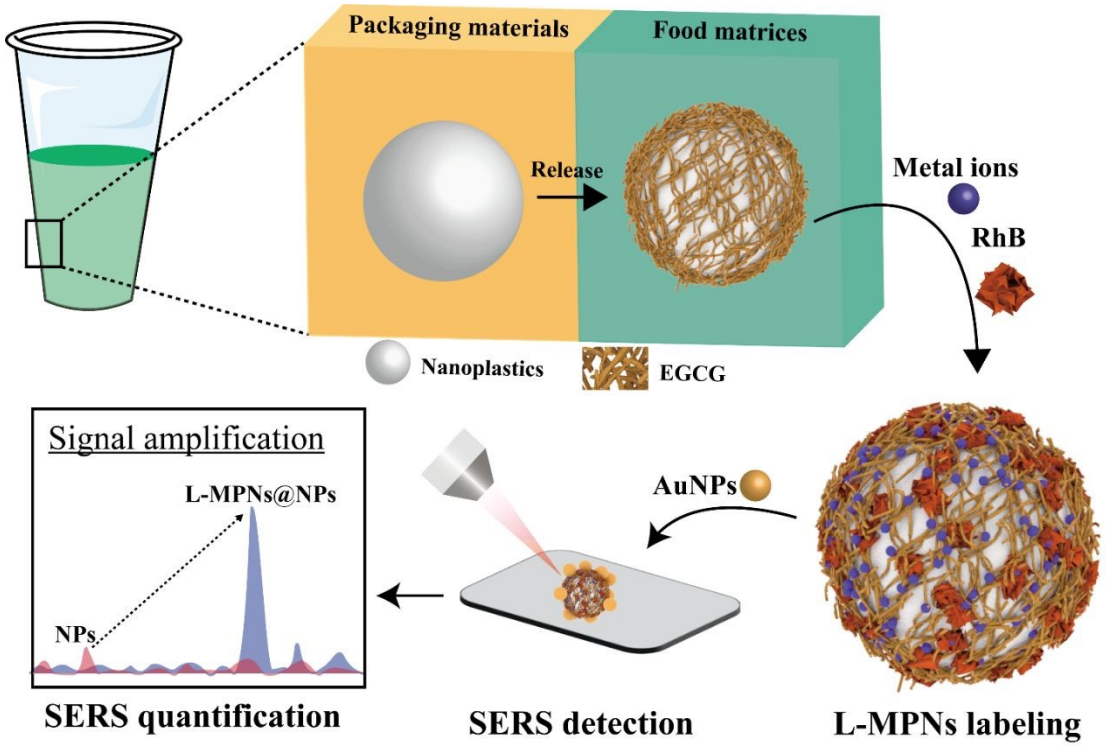

Scheme 1. Nanoplastics release and subsequent SERS detection during simulated tea drinks.

Experimental

Materials

Polystyrene nanoplastics with particle size of 500 nm were purchased from Phosphorex (Massachusetts, USA). EGCG (pharmaceutical secondary standard) and zinc chloride ($ZnCl_2$, >98%) was purchased from Sigma-Aldrich (Ontario, Canada). Rhodamine B (ACS reagent ≥99%) were purchased from VWR (Alberta, Canada). Dulbecco's Modified Eagle's Medium (DMEM-D5796; without pyruvate), phosphate buffered saline (PBS), penicillin/streptomycin antibiotics, 3-(4,5-diethylthiazol-2-yl)-2,5-diphenyltetrazolium bromide (MTT) and Dimethylsulfoxide (DMSO) were purchased from Sigma (St. Louis, MO, USA). Fetal bovine serum (FBS) was purchased from Gibco® (Grand Island, NY, USA). Transparent commercial polystyrene drinking cups (Ruisita, ASIN, B0B3GTSH4D) were purchased from Amazon.ca. The capacity of these clear mini dessert cups is 3 ounces; the dessert cups measure 3.1 inch/8 cm in height, 1.9 inch/4.7 cm in top diameter, and 1.3 inch/3.2 cm in bottom diameter. Gold nanoparticles (AuNPs, 50 nm ± 4 nm at a concentration of 1 mg/L) were purchased from nanoComposix (San Diego, CA, USA). Double-distilled water (DD water) was produced using a distillation system in the Food Nutrition and Health building at University of British Columbia (UBC), Vancouver

View Article Online
DOI: 10.1039/D6NR00796A

campus.

Preparation of L-MPNs@NPs

EGCG, Zn^{2+} metal ions, and RhB were selected as model reagents for the formation of L-MPNs. The preparation of L-MPNs labeled nanoplastics (L-MPNs@NPs) was carried out according to the protocols described in our prior research.[23] 500 nm PS NPs solutions were prepared to various concentrations of 0, 1.54×10^7, 7.7×10^7, 1.54×10^8, 7.7×10^8, 1.54×10^9, 7.7×10^9, 1.54×10^{10}, 7.7×10^{10}, 1.54×10^{11} n/mL. The nanoplastics concentration was provided by Phosphorex and further validated in our previous study using electrophoretic deposition–interferometric scattering (EPD-iSCAT).[24,25] Subsequently, EGCG was added into these suspensions to achieve a final concentration of 1 mg/mL. For the labeling process, 20 μL of $ZnCl_2$ (20 mM) and 20 μL of RhB (0.5 mM) were added to 960 μL of NPs-EGCG mixture, resulting in final concentrations of 400 μM Zn^{2+}, and 10 μM RhB. This mixture was thoroughly vortexed for 1 min and then centrifuged at 7500 rpm for 10 min. The supernatant was removed, and the precipitate was resuspended in 1 μL of DD water to prepare L-MPNs@NPs.

Characterization of L-MPNs@NPs

L-MPNs labeling on NPs was characterized using dynamic light scattering (DLS) and fluorescence measurements. DLS assessments for released NPs and L-MPNs@NPs samples were performed with a Litesizer 500 (Anton Paar, Graz, Austria). Fluorescence spectroscopy measurements were performed with a Tecan infinite 200Pro plate reader (excitation at 550 nm; emission at 595 nm) for released NPs labeled with RhB, Zn^{2+}/RhB, EGCG/RhB, and L-MPNs. Transmission Electron Microscopy (TEM) imaging was examined under a Hitachi H7600 TEM (Tokyo, Japan) at 80 kV for released NPs and NPs-EGCG mixtures.

Detection of NPs by the SERS

SERS was utilized to determine NPs labeled by L-MPNs. AuNPs solution was prepared by diluting stock solution to 0.5 mg/mL with DD water. A 1 μL droplet of AuNPs solution was applied onto aluminum foil, followed by the addition of an equal volume of the L-MPNs@NPs samples. Samples were allowed to air dry at room temperature for 10 min. Subsequently, SERS spectra were acquired at the periphery of the resultant coffee ring using a WP 785 ER Raman Spectrometer, which is equipped with a 785 nm excitation laser. The most reproducible signal from each sample was selected as the representative spectrum. Spectral acquisition was conducted under controlled conditions: the laser was set to a power of 450 mW, the integration time was fixed at 60 s, and spectra were recorded continuously over a range of 300–2008 cm^{-1}. The spectral data were

View Article Online
DOI: 10.1039/D6NR00796A

processed using boxcar smoothing and polynomial baseline corrections to enhance the signal clarity for improved accuracy.

MNPs release in a simulated tea consumption

EGCG was chosen as the representative bioactive polyphenol to simulate a simplified tea drink; The study utilized two primary thermal processes: boiling water and microwave heating water, with cold water control. For the boiling water treatments, different concentrations of EGCG (e.g., 0.1, 0.2, 0.4, 0.6 mg/mL) were added. In the microwave experiments, EGCG at the same concentrations used above were added to DD water at room temperature, followed by exposure to microwave heating (900 W) at varying time durations (e.g., 0, 15, 30, 60, 90, 120, 150, and 180 s). Following heating, all samples were cooled naturally at room temperature for approximately 30 min. The EGCG concentrations were adjusted to 1 mg/mL to maintain consistency across all samples. Subsequently, the release of NPs was measured by preparation of L-MPNs@NPs and then using SERS for quantification analysis.

Caco-2 cell viability exposed to NPs and NPs with EGCG.

Twenty-one-day old differentiated Caco-2 cells were used in this study to test the potential toxicity of NPs recovered from the plastic cups containing hot water. Cells were cultured in Dulbecco's modified Eagle's medium (DMEM) containing 4500 mg/L glucose and sodium bicarbonate, without L-glutamine and sodium pyruvate. Cell media also contained 10% FBS (Invitrogen, Canada), and 100 U/mL penicillin and 100 μg/mL of streptomycin (PS). Cells were cultured at 37 °C under a controlled atmosphere with 5% CO_2. The passage number for Caco-2 cells used in these experiments was 21–30. Caco-2 cells were seeded in 96-well plates at a density of 1×10^5 cells/cm^2, and the cell culture media were changed every 2–3 days for 21 days until differentiation.

Redox activity was assessed in differentiated Caco-2 cells as a measure of viability using the MTT assay (3-(4,5-dimethylthiazol-2-yl)-2,5-diphenyltetrazolium bromide) in 96-well plates. This assay is based on a redox mechanism, whereby NADPH-dependent enzymes in viable, healthy cells reduce MTT into formazan crystals, which are quantified by spectrophotometry.[26] The cells were first incubated with NPs and EGCG (0.1, 0.2, 0.4, 0.6 mg/mL) in cell culture medium. A positive control consisted of using NPs (1.54×10^6, 1.54×10^7, 1.54×10^8 and 1.54×10^9 n/mL) present with no EGCG. After 24 h of incubation, Caco-2 cells were washed with 100 μL of phosphate-buffered saline (PBS) three times and then incubated with 100 μL of DMEM containing 0.5 mg/mL MTT for 4 h in the dark at 37 °C. Dimethylsulfoxide (DMSO, 100 μL) was then added to the wells without discarding the DMEM, allowing formazan crystals to dissolve (for the measuring of absorbance) with another 30 min. Solubilized formazan in wells were quantified

View Article Online
DOI: 10.1039/D6NR00796A

by measuring absorbance at 540 nm, using the Multiskan Skyhigh Spectrophotometer (Thermolabsystem, Chantilly, VA, USA) with the following equation:

$$Viability\ (shown\ as\ \%\ of\ control) = \frac{Abs_{sample}}{Abs_{control}} * 100\%$$

Where Abs_{sample} = absorbance of cells that received treatment, and $Abs_{control}$ = absorbance by the cells that have not received treatment (negative control).

Statistical analysis

All experiments were performed using at least three technical replicates unless otherwise stated, and results are reported as mean ± standard deviation (SD). Statistical analyses were performed using OriginPro 2021 (OriginLab, Northampton, MA, USA). Comparisons between two groups were conducted using a two-tailed Student's *t*-test, and differences were considered statistically significant at $P < 0.05$. For SERS quantification, a polynomial regression model was used to generate the calibration curve relating nanoparticle concentration to the characteristic Raman peak intensity. The uncertainty reported in this study is based on the variability among replicate measurements; formal error propagation across the full analytical workflow, including calibration-model fitting and sample-processing steps, was not performed in the present study.

Results and Discussion

Formation of L-MPNs@MNPs

L-MPNs labeling strategy can be applied to PS plastic particles through a straightforward and simple self-assembly process.[14] For example, in our previous research, tannic acid /zirconium metal ions/RhB-based L-MPNs were used to effectively quantify commercial 500 nm PS NPs employing SERS measurements. In this study, we used EGCG and Zn^{2+} as model reagents to form L-MPNs on released MNPs from polystyrene cups. EGCG was chosen not to imply that it is generally superior to other polyphenols (e.g., tannic acid) for L-MPN formation, but because it allows the same food-relevant polyphenol to function both as a release-active component in the simulated tea system and as a ligand in the sensing platform. Figure 1a depicts plastics released from commercial plastic cups subjected to microwave heating for 90 seconds. The TEM image illustrates an amorphous morphology for particle sizes ranging from the micro- to the nano- scale. Subsequent fluorescence characterization (Figure 1b) of RhB interaction with the released plastic particles showed a significant reduction in fluorescence intensity when released MNPs were labeled with RhB, EGCG/RhB, and RhB/Zn^{2+}, in comparison to the labeling with L-MPNs ($P < 0.05$). This result underscores the critical role of the L-MPNs coordination network to enhance fluorescence labeling efficiency. DLS measurements provided additional information on the

View Article Online
DOI: 10.1039/D6NR00796A

particle size distribution of the MNPs before and after labeling with L-MPNs, indicating that released particles were primarily in the nanosized range. With post-labeling, a notable shift in the peak particle size from 307 nm to 586 nm occurred (Figure 1c), which was indicative of successful aggregation facilitation by the L-MPNs. Although micro-sized plastic particles were detected, the predominant fraction consisted of nanoparticles in the range of hundreds of nanometers, with a maximal intensity at 586 nm. Consequently, for SERS optimization and measurement, the released plastic particles were categorized as nanoplastics (NPs) with a size distribution centered around hundreds of nanometers.

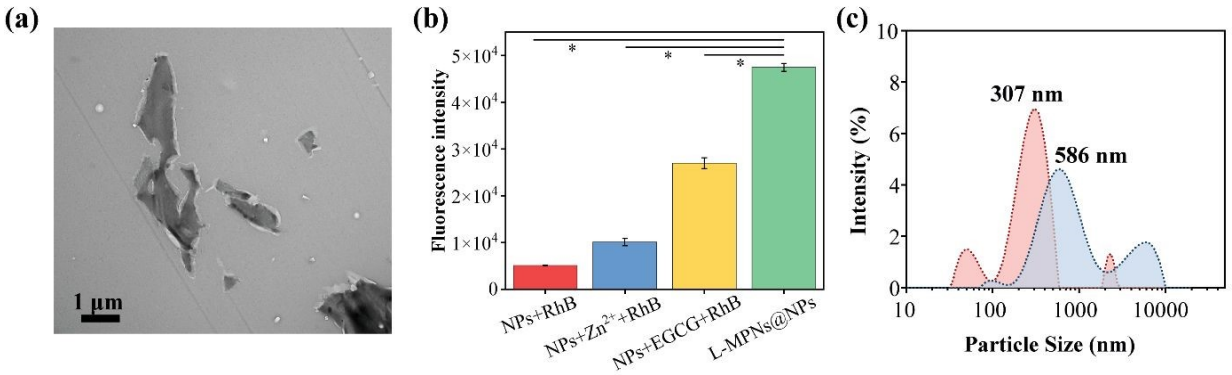

Figure 1. L-MPNs labeling of micro/nanoplastics. (a) TEM image of released plastic particles from plastic cups with microwave heating at 90 s (b) Fluorescence intensity measurements of released plastic particles labeled with RhB, Zn^{2+}/RhB, EGCG/RhB, and L-MPNs. (c) Particle size changes following the formation of L-MPNs@MNPs, in comparison to released MNPs alone. Data are represented as mean ± SD (n = 3 technical replicate). The asterisk (*) indicates a statistically significant difference ($P < 0.05$), as determined by the t-test.

SERS measurements of L-MPNs@NPs

To evaluate the efficacy of EGCG-based L-MPNs to quantify NPs utilizing SERS techniques, a series of SERS analyses was conducted on both the components of L-MPNs and NPs, both pre- and post-labelling with L-MPNs (Figure 2a). AuNPs served as the substrate for SERS which was selected for environmental stability,[27] PS NPs (500 nm) were chosen to represent NPs according to a known particle size, which closely approximated the plastics released from PS cups, as shown in Figure 1c. In the spectral analysis, AuNPs exhibited negligible signals across the spectrum. In contrast, RhB had distinctive peaks located at 1201, 1277, and 1357 cm^{-1}, respectively, with a very pronounced peak occurring at 1357 cm^{-1}, indicative of C-C stretching vibrations.[28] EGCG showed two peaks at 1340 and 1362 cm^{-1} , respectively, due to C-O vibrational modes.[29] The PS NPs displayed a characteristic peak at 998 cm^{-1}, attributed to ring-breathing modes. The synthesis of

View Article Online
DOI: 10.1039/D6NR00796A

L-MPNs induced alterations in these peak patterns, which were due to molecular interactions between RhB, EGCG, and Zn^{2+}, and attributed to coordination bonding between EGCG and Zn^{2+} and π–π interaction between RhB and EGCG.[30] However, the prominent peak presented at 1357 cm^{-1} was maintained, which served as the characteristic peak of L-MPNs for further quantitative analysis. Upon forming L-MPNs@NPs, the characteristic peak of PS at 998 cm^{-1} was substituted by a peak from the L-MPNs with an enhanced intensity at 1357 cm^{-1}. This finding showed the effectiveness of using RhB as a Raman reporter in EGCG based L-MPNs for improving the sensitivity of SERS detection of NPs.

Subsequent experiments to optimize Zn^{2+} concentrations were conducted to determine the pivotal role of metal ions in the efficacy of L-MPNs labeling.[14] Spectral analyses of L-MPNs@NPs (500 nm PS NPs at 1.54×10^9 n/mL) with varying Zn^{2+} concentrations were based on the intensity of the characteristic peak appearing at 1357 cm^{-1} (Figure 2b). The intensity of this peak was contrasted against control signals derived from L-MPNs without NPs, thus showing the effective SERS signal attributable to the presence of NPs (Figure 2c). This optimization experiment revealed that increasing Zn^{2+} concentration produced an enhancement in peak intensity. Low Zn^{2+} concentrations (0–10 mM) were insufficient for effective L-MPNs formation on NPs, whereas higher Zn^{2+} concentrations (40–100 mM) facilitated a denser coating, which facilitated greater binding activity with RhB molecules.[31] Excessive RhB binding caused aggregation and interfered with the optimal interaction between the RhB molecules and the SERS substrate (AuNPs), hence diminishing the SERS signal intensity. The Zn^{2+} concentration was optimized to 20 mM, as this concentration yielded the highest L-MPNs@NPs signal intensity. To ascertain the limit of detection (LOD) for NPs using this optimized EGCG-based L-MPNs method, a number of SERS assays were performed across various NPs concentrations. The results indicated a limit of detection (LOD) of 7.7×10^7 particles/mL, demonstrating a statistically significant difference ($p < 0.05$) between the sample group and lower concentration groups (Figure S1). Values exceeding the LOD for SERS signal intensity showed a positive correlation with increasing NPs concentration. A maximum concentration (1.53×10^{10}) resulted in a decrease in SERS intensity, likely due to the inhibition of the resonance Raman effect caused by aggregation.[32] Consequently, concentrations ranging from 7.7×10^7 to 7.7×10^{10} n/mL were used to establish a standard curve employing a polynomial regression model (Figure 2d & 2e, $R^2 = 0.979$), which outperformed liner fitting results (Figure S2, $R^2 = 0.969$). This model was used in the present study as a practical calibration framework for SERS-based quantification of L-MPN-labeled NPs. Orthogonal validation of the underlying quantification strategy was established in our previous work using electrophoretic deposition–interferometric scattering (EPD–iSCAT) measurements, whereas the current manuscript focuses on the EGCG-based application of this platform[33].

View Article Online
DOI: 10.1039/D6NR00796A

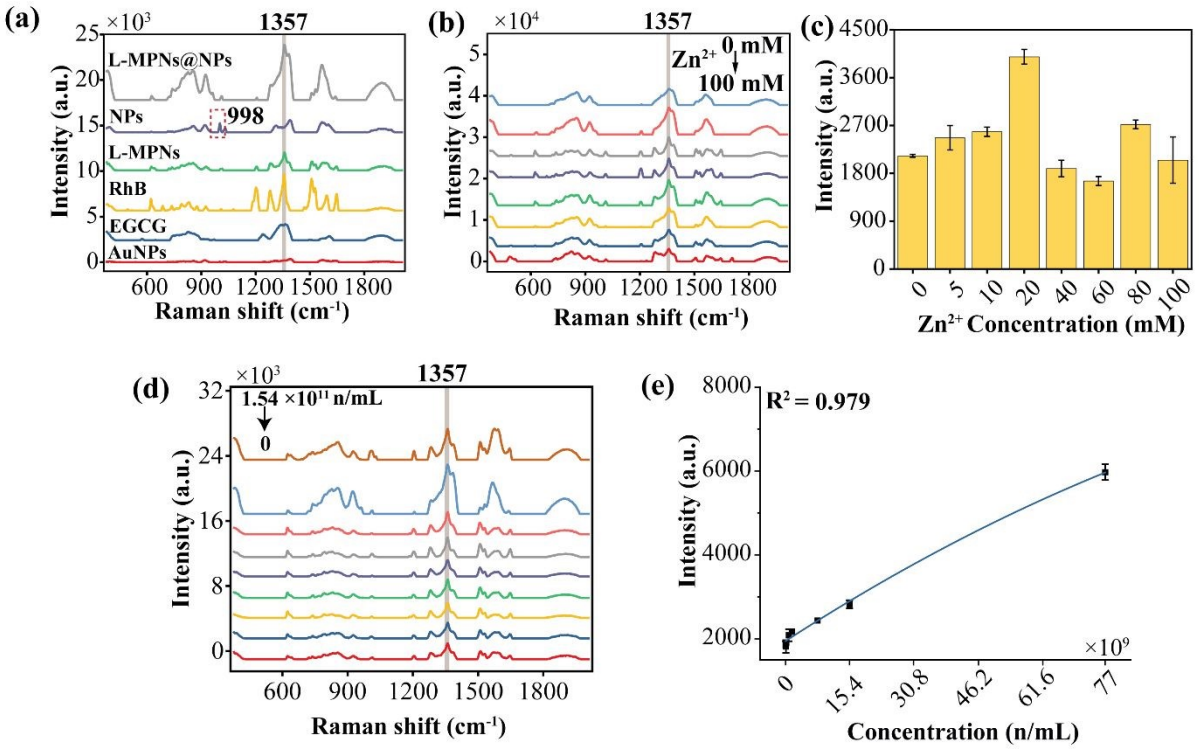

Figure 2. Optimization and Quantitative Analysis of Nanoplastics via SERS Measurements. (a) SERS spectra of AuNPs, EGCG, RhB, PS NPs, L-MPNs, and L-MPNs@NPs. (b) SERS spectra of L-MPNs@NPs with various Zn^{2+} concentrations (0, 5, 10, 20, 40, 60, 80, 100 mM). (c) Variation in the intensity of the characteristic peak at 1357 cm^{-1} for L-MPNs@NPs across these different Zn^{2+} concentrations. (d) SERS spectra of L-MPNs@NPs across various NPs concentrations (0, 1.54×10^7, 7.7×10^7, 1.54×10^8, 7.7×10^8, 1.54×10^9, 7.7×10^9, 1.54×10^{10}, 7.7×10^{10}, 1.54×10^{11} n/mL). (e) Investigation of the relationship between the concentration of NPs and the SERS characteristic peak intensity at 1357 cm^{-1} from L-MPNs employing polynomial regression model. The 500 nm PS NPs quantity concentration was controlled at 1.54×10^9 n/mL from Figure a-c. Data are represented as mean ± SD (n = 3 technical replicate).

Nanoplastics release from PS cups containing EGCG

Release of NPs from plastic products used for hot beverages has emerged as a potential health risk in daily life.[34–36] Our study investigated NPs release from PS cups by varying the pH levels from 5 to 9 and the concentrations of EGCG, a predominant polyphenol in tea, from 0 to 0.6 mg/mL.[37] Following the application of using both boiling water and water heated by microwave energy, respectively, samples were cooled and then labeled with L-MPNs before being quantified using SERS. We used EGCG in this experiment as both a phenolic ligand for L-MPNs formation and a representative tea polyphenol in a simplified tea model designed to isolate its specific contribution; this system does not reproduce the full compositional complexity of brewed tea[38].

View Article Online
DOI: 10.1039/D6NR00796A

The phenolic hydroxyl groups prevalent with EGCG did not show appreciable susceptibility to oxidation when exposed to boiling water and microwave heating conditions, respectively, as indicated by the fact that efficiency of L-MPNs labeling was not impacted (Figure S3). We maintained a consistent EGCG concentration of 1 mg/mL across different experimental groups to ensure uniform L-MPNs labeling conditions.

We first studied the effect of EGCG concentration and pH levels on nanoplastics release during boiling water heating. Our results indicate that low concentrations of EGCG (e.g., 0.1 and 0.2 mg/mL) in cups containing boiling water result in detectable, but minimal NPs release (0.5–1 $\times 10^8$ n/mL) across different pH levels. In contrast, significantly higher ($P<0.05$) NPs release (e.g., $4.26 \pm 0.32 \times 10^8$ n/mL) was observed when EGCG was present at higher concentrations (e.g., 0.4 to 0.6 mg/mL) (Figure 3a and Figure S4). NPs release was not detectable in cold water treatment at 30 min because the released NPs are below the LOD of our sensing method and direct SERS detection without L-MPNs (Figure S5). The ability of EGCG to facilitate NP release is attributed to the high affinity of catechol or galloyl groups in polyphenols, which can bind with various nanoplastics.[19,39] For example, electron-rich π-conjugated orbitals of aromatic rings in PS facilitate the formation of π-π interactions with polyphenol molecules. Furthermore, polyphenols rich with aromatic groups have hydrophobic interactions with various MNPs, such as PS, polyethylene (PE), polyvinyl chloride (PVC), and polypropylene (PP).[40] Under alkaline conditions (e.g., pH 9), higher concentrations of EGCG (0.6 mg/mL) resulted in more substantial NPs release compared to acidic and neutral conditions. In alkaline conditions, phenolic hydroxyl groups in polyphenols deprotonate to form phenoxide ions. The deprotonation increases the electron density on the phenoxide ion, potentially enhancing its ability to participate in π-π interactions with PS nanoplastics[41,42], thereby promoting NPs release. TEM images confirmed the interaction between PS and EGCG, further substantiating the enhanced release of NPs (Figure 3b).

Applying microwave energy to heat water in plastic cups notably lead to higher NPs release at neutral conditions (pH 7), compared to boiling heating conditions (Figure 3a, Figure 3c and Figure S6). This effect can be attributed to the susceptibility of PS polymer chains to breakdown into smaller fragments creating microcracks or fissures in the plastic cup that will facilitate NPs leaching into the water.[43] The effect of EGCG to contribute to NPs release after 30-60 s exposure to microwave energy was significantly greater than the zero time control, thus denoting a significant interaction ($P<0.05$) with EGCG concentration and time of microwave heating on NPs release. Note that our SERS assay could not detect EGCG-facilitated NPs' release below LOD in control and with very short 15-second microwave heating. The greatest NPs release (e.g., $6.47 \pm 0.11 \times 10^9$ n/mL) was facilitated by the presence of EGCG occurred at 0.6 mg/mL, which also

View Article Online
DOI: 10.1039/D6NR00796A

indicated that a higher concentration of EGCG induced more NPs release. The analysis results of reusable cups are significant as it reflects real-world tea drinking behaviors, where individuals often refill cups multiple times with hot water. We aimed to understand the implications of such practices on NPs release. The findings indicate that reusing PS cups treated with heating reaching boiling showed a linear increase in NPs measurements after 4 cycles, followed by a small decline thereafter (Figure 3d and Figure S7). Again, this was most likely due to damage to the uniform surface typical of PS cups reused and exposed to repeated boiling treatments.

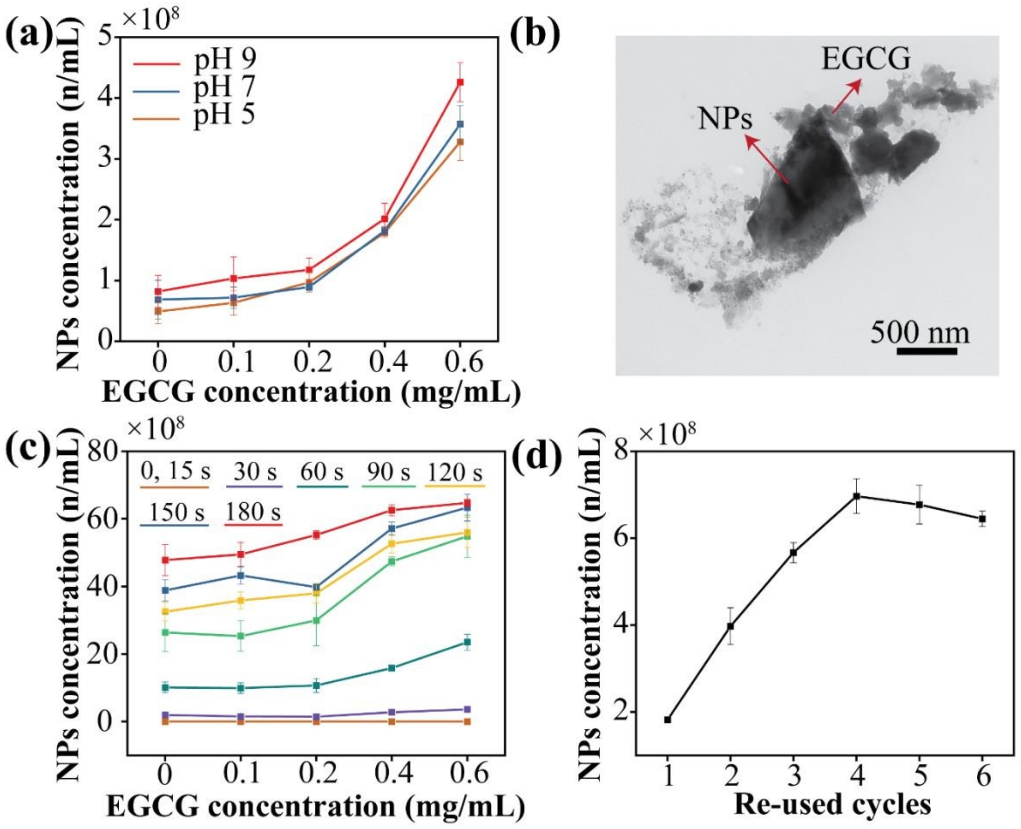

Figure 3. NPs release from water samples containing EGCG. (a) NPs release across various EGCG concentrations (0, 0.1, 0.2, 0.4, 0.6 mg/mL) and pH conditions (5, 7, 9) in boiling water. (b) TEM images of released NPs at an EGCG concentration of 0.4 mg/mL. (c) NPs release at different EGCG concentrations (0, 0.1, 0.2, 0.4, 0.6 mg/mL) subjected to various microwave heating durations (0, 15, 30, 60, 90, 120, 150, 180 s). (d) NPs release over various reuse cycles. Data are represented as mean ± SD (n = 3 technical replicate). No detectable NPs were recovered from cold water treatments.

Potential Caco-2 cell cytotoxicity

View Article Online
DOI: 10.1039/D6NR00796A

Twenty-one day, differentiated Caco-2 cells served as a representative *in vitro* model for the human intestinal epithelium, enabling the evaluation of the cytotoxic potential of NPs. In this study, we employed changes in Caco-2 cell redox status to assess cell viability when exposed to NPs derived from 500 nm PS. Our findings in Figure 4a indicate that low NPs concentrations (1.54×10^7 and 1.54×10^6 n/mL) do not significantly alter cell viability from 100% MTT control. Conversely, higher PS NPs concentrations (e.g., 1.54×10^8 and 1.54×10^9 n/mL), decreased MTT-redox values to $91.46 \pm 3.02\%$ and $82.09 \pm 2.39\%$, respectively ($P<0.05$). These results corroborate previous findings that reported elevated concentrations of NPs are cytotoxic to Caco-2 cells[44], through mechanisms that are associated with oxidative stress, inflammatory responses, and disruption of cellular functions.[45] The very small size of NPs likely facilitates penetration and accumulation within cellular structures, exacerbating a toxic effect. Examining the effect of pH (e.g., 5-9) on the toxicity of released NPs exposed to microwave heating (90 s) and boiling conditions showed that pH was not a factor in increasing potential toxicity of NPs. (Figure 4b). Comparing microwave heating with direct heat boiling showed that the former resulted in a greater release of NPs ($P<0.05$) and, thus, higher cytotoxicity.

We also explored the potential beneficial effects of adding tea polyphenol, EGCG to potentially reduce Caco-2 cell toxicity during microwave heating and boiling water conditions, respectively. Increasing EGCG concentrations in two heated water treatments significantly enhanced cell MTT responses ($P<0.05$) (Figure 4c). EGCG is a known antioxidant capable of scavenging reactive oxygen species and modulating cellular redox balance; in addition, its phenolic structure enables interactions with nanoplastics (e.g., π–π interactions and surface adsorption), which may alter particle surface properties and reduce their biological interactions.[46] When PS cups were microwaved, NPs release in heated water occurred and EGCG at low concentrations (0.1 mg/mL) were insufficient to mitigate the cytotoxic effects induced by NPs. However, at higher concentrations of EGCG (0.2, 0.4, 0.6 mg/mL), reduced Caco-2 cell toxicity was replaced to above 100% of control. In contrast with boiling water, where NP release was low, the toxic impact of released NPs on intestinal cell redox was minimal. Thus, EGCG increased the MTT response under the tested conditions; this preliminary effect may be associated with the known antioxidant activity of EGCG and/or with EGCG–nanoplastic interactions that alter particle surface behavior, such as binding and aggregation, thereby potentially reducing biological interactions[47,48]. However, these mechanisms require direct verification in future work. Additional endpoints, including ROS, TEER, and LDH will be important in future studies to provide mechanistic insight. These observations underscore the importance of accounting for both the source of plastic exposure and the presence of polyphenolic compounds, such as ECGC when assessing the effect of using microwave heating on tea beverages.

View Article Online
DOI: 10.1039/D6NR00796A

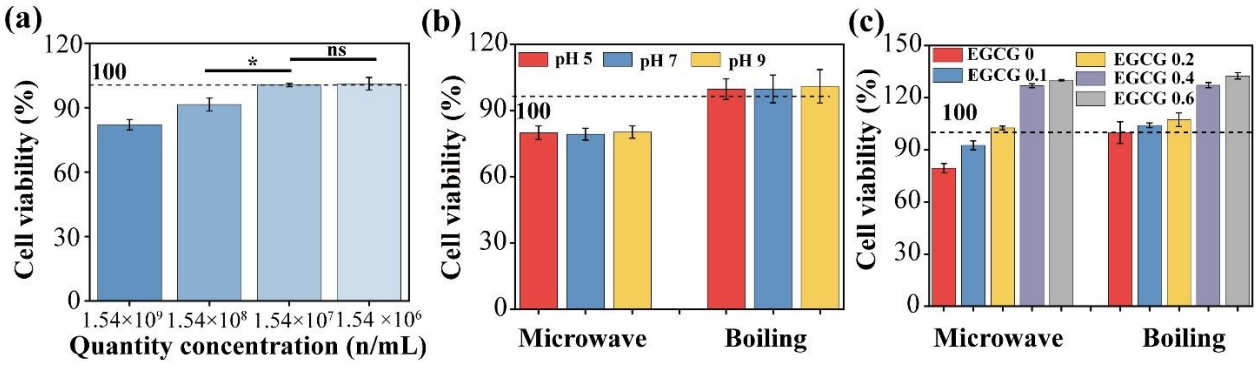

Figure 4. Influence of PS NPs and EGCG on the viability of Caco-2 cells. (a) Cell viability following exposure to commercially 500 nm PS NPs at concentrations of 1.54×10^6, 1.54×10^7, 1.54×10^8, and 1.54×10^9/mL. (b) Cell viability following exposure to released NPs at different pH levels (5, 7, 9) under microwave heating and boiling conditions. (c) Cell viability following exposure to released NPs at different EGCG levels (0, 0.1, 0.2, 0.4, 0.6 mg/mL) under microwave heating and boiling conditions. Data are represented as mean ± SD (n = 3 technical replicate). Values were determined when comparing with cold water control (100%). The label "ns" denotes no significant difference, whereas the asterisk "*" signifies a statistically significant difference with a p-value < 0.05, as determined by the t-test.

Dietary intake pathways and food–plastic interactions: implications for nanoplastic exposure, food safety, and environmental health

MNPs can enter the human diet from various sources, such as contaminated food products, food processing, and packaging materials. For example, seafood accumulates MNPs from contaminated marine environments, serving as a key food source. Drinking water and beverages contained in plastic bottles also contributes to exposure due to the release of MNPs. Similarly, heating food in plastic containers, particularly in microwaves, can accelerate the release of microplastics into foods, such as, ready to eat meals). Figure 5-top panel illustrates the estimated daily dietary intake of microplastics across different countries. Regions with higher plastic consumption in food packaging, seafood-heavy diets, and greater environmental plastic pollution tend to show higher microplastics ingestion rates.[43] For instance, countries in Southeast Asia, such as Indonesia, Malaysia, and the Philippines, report the highest microplastic ingestion rates. In fact, Indonesians eat about 15 grams of microplastics every month, more than any other country and by comparison, dietary intake in North America was roughly 2.2 grams per month. As the growing health and environmental concerns surrounding MNPs, understanding the foods consumed that are also contained in plastic packaging, and the factors that may influence this process is critical for risk mitigation and developing effective strategies.

View Article Online
DOI: 10.1039/D6NR00796A

We provide new evidence that the major tea polyphenol, EGCG, significantly influences nanoplastic release under thermal exposure. Our study highlights significant implications for food safety and public health by demonstrating that polyphenol-rich beverages, such as tea containing EGCG, can enhance nanoplastics release from plastic cups, particularly under microwave heating. This finding could challenge existing food packaging safety assessments, which primarily focus on chemical additives or nanomaterial migration limits without accounting for real-world interactions between food components and plastic materials. From a practical perspective, our findings contribute to ongoing discussions about food packaging safety and consumer practices. While plastics labeled as 'microwave-safe" are widely used, our study suggests that other factors, such as heating conditions, food composition, and repeated use could also influence the extent of MNPs release.

Interestingly, while EGCG enhanced NP release, we also demonstrated protective antioxidant effects against NP-induced cellular stress in our in vitro intestinal cell-based model. This raises important questions about how food matrix components interact with nanoplastics in the digestive system and whether the interaction could affect NP intestinal health. It is also important to explore whether other dietary antioxidants have similar protective effects and how different types of plastics behave under various food preparation conditions. Our research findings emphasize the importance of a broader understanding of real-world food-plastic interactions in assessing MNP dietary intake and highlight the need for further research on dietary strategies or common practices to mitigate NP potential toxicity. An example of the latter is the correlation between the practice of regular hot tea consumption using reusable plastic cups in Asia. Here the daily intake of both EGCG from tea and exposure to ingested NPs are cumulative and interconnected.

The lower panel of Figure 5 presents a flowchart detailing the factors that impact MNP release from plastic packaging, the potential health and environmental consequences, and pathways to developing safer packaging solutions. Several key factors contribute to MNP migration into food, including the composition of the food/beverage, the type and condition of plastic packaging, and environmental conditions such as heat, acidity, and UV exposure. Once ingested, these particles may cause negative environmental impacts and pose health risks, such as oxidative stress and inflammation, which are linked to broader concerns regarding chronic, long-term human exposure. To support risk assessment, further research innovation is necessary for studying the interactions between food/beverage components and packaging materials under real-world conditions. A better understanding of these factors could better support the development of safer and more sustainable packaging materials while ensuring that food/beverage preparation methods minimize unintended exposure to MNPs. Collaborative efforts between researchers, industry professionals, and

View Article Online
DOI: 10.1039/D6NR00796A

regulatory bodies may help guide future innovations in food packaging and food safety assessments, ultimately benefiting both consumer health and environmental sustainability.

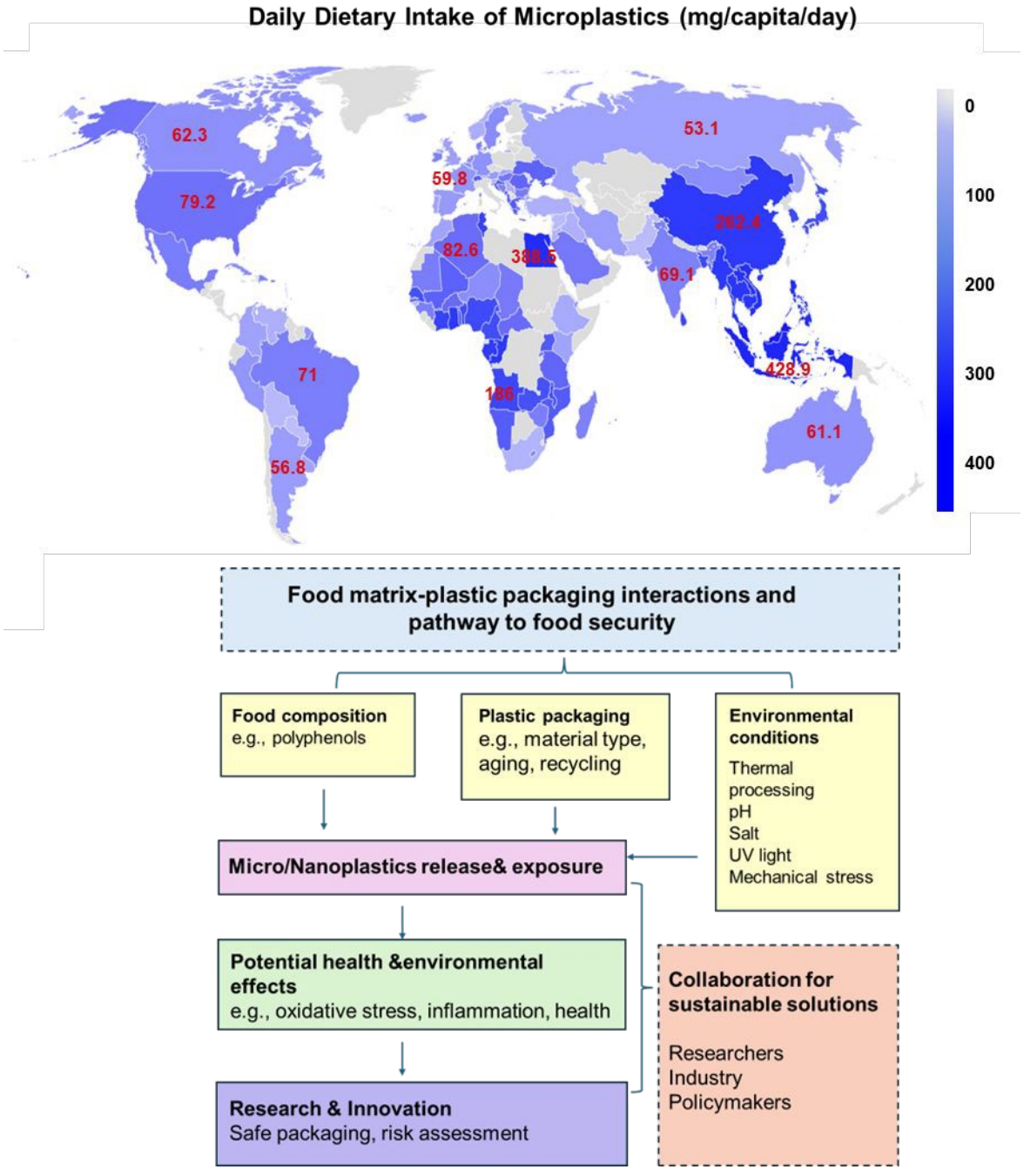

Figure 5. Global dietary intake of microplastics (mg/capital/day) and conceptual framework illustrating the interactions between food matrices and plastic packaging and their implications for

View Article Online
DOI: 10.1039/D6NR00796A

food safety and security. The map shows estimated daily microplastic intake across different regions, emphasizing the worldwide prevalence of plastic particle exposure. The schematic below highlights key contributing factors, including food composition (e.g., polyphenols), packaging characteristics (e.g., material type, aging, recycling), and environmental conditions (e.g., thermal processing, pH, UV light, mechanical stress), that influence micro/nanoplastic release and human exposure. Resulting health and environmental effects, such as oxidative stress and inflammation, highlight the need for continued research and innovation in safe packaging design, risk assessment, and cross-sector collaboration among researchers, industry, and policymakers to develop sustainable solutions.

Conclusions

This study establishes a robust analytical framework for quantifying nanoplastics released from plastic cups containing polyphenols during heating treatments. We provide new evidence that the major tea polyphenol, EGCG, significantly influences nanoplastic release under thermal exposure. EGCG greatly increased nanoparticle release, particularly during microwave heating, while simultaneously mitigating nanoplastic-induced cytotoxicity in differentiated Caco-2 cells. Repeated use of PS cups in boiling water led to cumulative nanoparticle release, emphasizing long-term exposure concerns associated with plastic reuse. These findings reveal complex chemical and physical interactions among beverage composition, packaging materials, and environmental factors that shape nanoplastic release and exposure pathways. By integrating advanced SERS detection with toxicological assessment, this work advances current understanding of MNPs exposure mechanisms at the food–environment interface. The study provides novel insights into contaminant release dynamics, exposure risk assessment, and the need for safer, more sustainable materials in food contact applications. Future research should focus on the interplay between diverse food components and packaging materials, which will be critical to mitigating unintended nanoplastic exposure and promoting public and environmental health.

Author contributions

The manuscript was written through contributions of all authors. All authors have given approval to the final version of the manuscript.

Conflicts of interest

There are no conflicts to declare.

View Article Online
DOI: 10.1039/D6NR00796A

Data availability

The data supporting this article have been included as part of the Supplementary Information (SI). Supporting information: SERS detection of nanoplastics, effect of heating on SERS detection, and raw SERS spectra of NP release across different conditions (PDF). See DOI:

Acknowledgements

This work was supported by the UBC Faculty of Land and Food Systems/Start Up Funds (AWD-020249 UBCLANDF 2022), Natural Sciences and Engineering Research Council of Canada (NSERC) Discovery Grants Program (RGPIN-2023-04100) and NSERC Discovery Grants Program-Discovery Launch Supplement (DGECR-2023-00386). We acknowledge the Canada Foundation for Innovation and John R. Evans Leaders Fund (CFI-JELF #44768), and the British Columbia Knowledge Development Fund (BCKDF). We also thank V. Pringle from the UBC Bioimaging Facility (RRID: SCR_021304) for completing TEM.

View Article Online
DOI: 10.1039/D6NR00796A

References

(1) Li, W.; Wu, C.; Xiong, Z.; Liang, C.; Li, Z.; Liu, B.; Cao, Q.; Wang, J.; Tang, J.; Li, D. Self-Driven Magnetorobots for Recyclable and Scalable Micro/Nanoplastic Removal from Nonmarine Waters. *Science Advances* **2022**, *8* (45), eade1731. https://doi.org/10.1126/sciadv.ade1731.

(2) Ye, H.; Zheng, X.; Yang, H.; Kowal, M.; Seifried, T.; Singh, G. P.; Aayush, K.; Gao, G.; Grant, E.; Kitts, D.; Yada, R.; Yang, T. Rapid Detection of Micro/Nanoplastics Via Integration of Luminescent Metal Phenolic Networks Labeling and Quantitative Fluorescence Imaging in A Portable Device. ChemRxiv September 29, 2023. https://doi.org/10.26434/chemrxiv-2023-jnbm1.

(3) Stubbins, A.; Law, K. L.; Muñoz, S. E.; Bianchi, T. S.; Zhu, L. Plastics in the Earth System. *Science* **2021**, *373* (6550), 51–55. https://doi.org/10.1126/science.abb0354.

(4) Yin, K.; Wang, Y.; Zhao, H.; Wang, D.; Guo, M.; Mu, M.; Liu, Y.; Nie, X.; Li, B.; Li, J.; Xing, M. A Comparative Review of Microplastics and Nanoplastics: Toxicity Hazards on Digestive, Reproductive and Nervous System. *Science of The Total Environment* **2021**, *774*, 145758. https://doi.org/10.1016/j.scitotenv.2021.145758.

(5) Hu, M.; Palić, D. Micro- and Nano-Plastics Activation of Oxidative and Inflammatory Adverse Outcome Pathways. *Redox Biology* **2020**, *37*, 101620. https://doi.org/10.1016/j.redox.2020.101620.

(6) Fang, C.; Luo, Y.; Naidu, R. Microplastics and Nanoplastics Analysis: Options, Imaging, Advancements and Challenges. *TrAC Trends in Analytical Chemistry* **2023**, *166*, 117158. https://doi.org/10.1016/j.trac.2023.117158.

(7) Shi, K.; Zhang, H.; Yang, Y.; Huang, Y.; Gao, J.; Zhang, J.; Kan, G.; Jiang, Y.; Jiang, J. Efficient Extraction and Analysis of Nanoplastics by Ionic Liquid-Assisted Cloud-Point Extraction Coupled with Electromagnetic Heating Pyrolysis Mass Spectrometry. *Anal. Chem.* **2024**. https://doi.org/10.1021/acs.analchem.3c05208.

(8) Cai, H.; Xu, E. G.; Du, F.; Li, R.; Liu, J.; Shi, H. Analysis of Environmental Nanoplastics: Progress and Challenges. *Chemical Engineering Journal* **2021**, *410*, 128208. https://doi.org/10.1016/j.cej.2020.128208.

(9) Zhang, X.; Shi, K.; Liu, Y.; Chen, Y.; Yu, K.; Wang, Y.; Zhang, H.; Jiang, J. Rapid and Efficient Method for Assessing Nanoplastics by an Electromagnetic Heating Pyrolysis Mass Spectrometry. *Journal of Hazardous Materials* **2021**, *419*, 126506. https://doi.org/10.1016/j.jhazmat.2021.126506.

(10) Xiang, C.; Gao, J.; Ye, H.; Ren, G.; Ma, X.; Xie, H.; Fang, S.; Lei, Q.; Fang, W. Development of Ovalbumin-Pectin Nanocomplexes for Vitamin D3 Encapsulation: Enhanced Storage Stability and Sustained Release in Simulated Gastrointestinal Digestion. *Food Hydrocolloids* **2020**, *106*, 105926. https://doi.org/10.1016/j.foodhyd.2020.105926.

(11) Ye, H.; Chen, T.; Huang, M.; Ren, G.; Lei, Q.; Fang, W.; Xie, H. Exploration of the Microstructure and Rheological Properties of Sodium Alginate-Pectin-Whey Protein Isolate Stabilized B-Carotene Emulsions: To Improve Stability and Achieve Gastrointestinal

View Article Online
DOI: 10.1039/D6NR00796A

Sustained Release. *Foods* **2021**, *10* (9), 1991. https://doi.org/10.3390/foods10091991.

(12) Li, Z.; Han, K.; Zhang, A.; Wang, T.; Yan, Z.; Ding, Z.; Shen, Y.; Zhang, M.; Zhang, W. Honeycomb-like AgNPs@TiO2 Array SERS Sensor for the Quantification of Micro/Nanoplastics in the Environmental Water Samples. *Talanta* **2024**, *266*, 125070. https://doi.org/10.1016/j.talanta.2023.125070.

(13) Leonard, J.; Koydemir, H. C.; Koutnik, V. S.; Tseng, D.; Ozcan, A.; Mohanty, S. K. Smartphone-Enabled Rapid Quantification of Microplastics. *Journal of Hazardous Materials Letters* **2022**, *3*, 100052. https://doi.org/10.1016/j.hazl.2022.100052.

(14) Ye, H.; Gao, G.; Yang, T. Quantitative and Rapid Detection of Nanoplastics Labeled by Luminescent Metal Phenolic Networks Using Surface Enhanced Raman Scattering. Rochester, NY January 26, 2024. https://doi.org/10.2139/ssrn.4696808.

(15) Lin, Z.; Zhou, J.; Qu, Y.; Pan, S.; Han, Y.; Lafleur, R. P. M.; Chen, J.; Cortez-Jugo, C.; Richardson, J. J.; Caruso, F. Luminescent Metal-Phenolic Networks for Multicolor Particle Labeling. *Angewandte Chemie International Edition* **2021**, *60* (47), 24968–24975. https://doi.org/10.1002/anie.202108671.

(16) Hernandez, L. M.; Xu, E. G.; Larsson, H. C. E.; Tahara, R.; Maisuria, V. B.; Tufenkji, N. Plastic Teabags Release Billions of Microparticles and Nanoparticles into Tea. *Environ. Sci. Technol.* **2019**, *53* (21), 12300–12310. https://doi.org/10.1021/acs.est.9b02540.

(17) Hernandez, L. M.; Xu, E. G.; Larsson, H. C. E.; Tahara, R.; Maisuria, V. B.; Tufenkji, N. Plastic Teabags Release Billions of Microparticles and Nanoparticles into Tea. *Environ. Sci. Technol.* **2019**, *53* (21), 12300–12310. https://doi.org/10.1021/acs.est.9b02540.

(18) Lee, D.-H.; Kim, W.-H.; Lee, K.; Na, I.; Fu, X.; Jeong, H. W.; Chung, J.-O.; Roh, J.; Kim, W.; Shim, S.-M. Green Tea Extracts Rich in Epicatechins Inducing Aggregation and Inhibiting Absorption of Amine Surface Functionalized Polystyrene Microplastics *in Vitro* Mimick System. *Journal of Hazardous Materials Advances* **2024**, *15*, 100437. https://doi.org/10.1016/j.hazadv.2024.100437.

(19) Xie, H.; Luo, X.; Gao, Y.; Huang, M.; Ren, G.; Zhou, R.; Sun, Y.; Ye, H.; Lei, Q.; Fang, W.; Xu, Y.-Q. Co-Encapsulation of *Lactobacillus Plantarum* and EGCG: A Promising Strategy to Increase the Stability and Lipid-Lowering Activity. *Food Hydrocolloids* **2024**, *151*, 109768. https://doi.org/10.1016/j.foodhyd.2024.109768.

(20) Hu, C.; Kitts, D. D. Evaluation of Antioxidant Activity of Epigallocatechin Gallate in Biphasic Model Systems in Vitro. *Mol Cell Biochem* **2001**, *218* (1), 147–155. https://doi.org/10.1023/A:1007220928446.

(21) Arts, I. C. W.; van de Putte, B.; Hollman, P. C. H. Catechin Contents of Foods Commonly Consumed in The Netherlands. 2. Tea, Wine, Fruit Juices, and Chocolate Milk. *J. Agric. Food Chem.* **2000**, *48* (5), 1752–1757. https://doi.org/10.1021/jf000026+.

(22) Atanasov, A. G.; Sabharanjak, S. M.; Zengin, G.; Mollica, A.; Szostak, A.; Simirgiotis, M.; Huminiecki, Ł.; Horbanczuk, O. K.; Nabavi, S. M.; Mocan, A. Pecan Nuts: A Review of Reported Bioactivities and Health Effects. *Trends in Food Science & Technology* **2018**, *71*, 246–257. https://doi.org/10.1016/j.tifs.2017.10.019.

(23) Ye, H.; Esfahani, E. B.; Chiu, I.; Mohseni, M.; Gao, G.; Yang, T. Quantitative and Rapid

View Article Online
DOI: 10.1039/D6NR00796A

Detection of Nanoplastics Labeled by Luminescent Metal Phenolic Networks Using Surface-Enhanced Raman Scattering. *Journal of Hazardous Materials* **2024**, *470*, 134194. https://doi.org/10.1016/j.jhazmat.2024.134194.

(24) Ye, H.; Zheng, X.; Yang, H.; Kowal, M. D.; Seifried, T. M.; Singh, G. P.; Aayush, K.; Gao, G.; Grant, E.; Kitts, D.; Yada, R. Y.; Yang, T. Cost-Effective and Wireless Portable Device for Rapid and Sensitive Quantification of Micro/Nanoplastics. *ACS Sens.* **2024**, *9* (9), 4662–4670. https://doi.org/10.1021/acssensors.4c00957.

(25) Kowal, M. D.; Seifried, T. M.; Brouwer, C. C.; Tavakolizadeh, H.; Olsén, E.; Grant, E. Electrophoretic Deposition Interferometric Scattering Mass Photometry. *ACS Nano* **2024**, *18* (15), 10388–10396. https://doi.org/10.1021/acsnano.3c09221.

(26) Kumar, P.; Nagarajan, A.; Uchil, P. D. Analysis of Cell Viability by the MTT Assay. *Cold Spring Harb Protoc* **2018**, *2018* (6), pdb.prot095505. https://doi.org/10.1101/pdb.prot095505.

(27) Wu, L.-A.; Li, W.-E.; Lin, D.-Z.; Chen, Y.-F. Three-Dimensional SERS Substrates Formed with Plasmonic Core-Satellite Nanostructures. *Sci Rep* **2017**, *7* (1), 13066. https://doi.org/10.1038/s41598-017-13577-9.

(28) Huh, S.; Park, J.; Kim, Y. S.; Kim, K. S.; Hong, B. H.; Nam, J.-M. UV/Ozone-Oxidized Large-Scale Graphene Platform with Large Chemical Enhancement in Surface-Enhanced Raman Scattering. *ACS Nano* **2011**, *5* (12), 9799–9806. https://doi.org/10.1021/nn204156n.

(29) Zhao, Y.; Xu, L.; Kong, F.; Yu, L. Design and Preparation of Poly(Tannic Acid) Nanoparticles with Intrinsic Fluorescence: A Sensitive Detector of Picric Acid. *Chemical Engineering Journal* **2021**, *416*, 129090. https://doi.org/10.1016/j.cej.2021.129090.

(30) Lin, Z.; Zhou, J.; Qu, Y.; Pan, S.; Han, Y.; Lafleur, R. P. M.; Chen, J.; Cortez-Jugo, C.; Richardson, J. J.; Caruso, F. Luminescent Metal-Phenolic Networks for Multicolor Particle Labeling. *Angewandte Chemie International Edition* **2021**, *60* (47), 24968–24975. https://doi.org/10.1002/anie.202108671.

(31) Mazaheri, O.; Alivand, M. S.; Zavabeti, A.; Spoljaric, S.; Pan, S.; Chen, D.; Caruso, F.; Suter, H. C.; Mumford, K. A. Assembly of Metal–Phenolic Networks on Water-Soluble Substrates in Nonaqueous Media. *Advanced Functional Materials* **2022**, *32* (24), 2111942. https://doi.org/10.1002/adfm.202111942.

(32) Bell, S. E. J.; Sirimuthu, N. M. S. Quantitative Surface-Enhanced Raman Spectroscopy. *Chem. Soc. Rev.* **2008**, *37* (5), 1012. https://doi.org/10.1039/b705965p.

(33) Ye, H.; Jiang, S.; Yan, Y.; Zhao, B.; Grant, E.; Kitts, D.; Yada, R.; Pratap-Singh, A.; Baldelli, A.; Yang, T. Integrating Metal Phenolic Networks-Mediated Separation and Machine Learning-Aided SERS for High-Precision Quantification and Classification of Nanoplastics. ChemRxiv July 5, 2024. https://doi.org/10.26434/chemrxiv-2024-kn4zj.

(34) Liu, G.; Wang, J.; Wang, M.; Ying, R.; Li, X.; Hu, Z.; Zhang, Y. Disposable Plastic Materials Release Microplastics and Harmful Substances in Hot Water. *Science of The Total Environment* **2022**, *818*, 151685. https://doi.org/10.1016/j.scitotenv.2021.151685.

(35) Hernandez, L. M.; Xu, E. G.; Larsson, H. C. E.; Tahara, R.; Maisuria, V. B.; Tufenkji, N. Plastic Teabags Release Billions of Microparticles and Nanoparticles into Tea. *Environ. Sci. Technol.* **2019**, *53* (21), 12300–12310. https://doi.org/10.1021/acs.est.9b02540.

View Article Online
DOI: 10.1039/D6NR00796A

(36) Hee, Y. Y.; Weston, K.; Suratman, S. The Effect of Storage Conditions and Washing on Microplastic Release from Food and Drink Containers. *Food Packaging and Shelf Life* **2022**, *32*, 100826. https://doi.org/10.1016/j.fpsl.2022.100826.

(37) Zhen-Yu Chen, *; Qin Yan Zhu, †; David Tsang, † and; Huang‡, Y. *Degradation of Green Tea Catechins in Tea Drinks*. ACS Publications. https://doi.org/10.1021/jf000877h.

(38) Xie, H.; Luo, X.; Gao, Y.; Huang, M.; Ren, G.; Zhou, R.; Sun, Y.; Ye, H.; Lei, Q.; Fang, W.; Xu, Y.-Q. Co-Encapsulation of *Lactobacillus Plantarum* and EGCG: A Promising Strategy to Increase the Stability and Lipid-Lowering Activity. *Food Hydrocolloids* **2024**, *151*, 109768. https://doi.org/10.1016/j.foodhyd.2024.109768.

(39) Zhao, W.; Liang, X.; Wang, X.; Wang, S.; Wang, L.; Jiang, Y. Chitosan Based Film Reinforced with EGCG Loaded Melanin-like Nanocomposite (EGCG@MNPs) for Active Food Packaging. *Carbohydrate Polymers* **2022**, *290*, 119471. https://doi.org/10.1016/j.carbpol.2022.119471.

(40) Wang, Y.; Wang, M.; Wang, Q.; Wang, T.; Zhou, Z.; Mehling, M.; Guo, T.; Zou, H.; Xiao, X.; He, Y.; Wang, X.; Rojas, O. J.; Guo, J. Flowthrough Capture of Microplastics through Polyphenol-Mediated Interfacial Interactions on Wood Sawdust. *Advanced Materials* **2023**, *35* (36), 2301531. https://doi.org/10.1002/adma.202301531.

(41) Zhu, H.; Ma, X.; Kong, J. Y.; Zhang, M.; Kenttämaa, H. I. Identification of Carboxylate, Phosphate, and Phenoxide Functionalities in Deprotonated Molecules Related to Drug Metabolites via Ion–Molecule Reactions with Water and Diethylhydroxyborane. *J. Am. Soc. Mass Spectrom.* **2017**, *28* (10), 2189–2200. https://doi.org/10.1007/s13361-017-1713-0.

(42) Zhang, L.; Liu, Y.; Wang, Y. Deprotonation Mechanism of Methyl Gallate: UV Spectroscopic and Computational Studies. *International Journal of Molecular Sciences* **2018**, *19* (10), 3111. https://doi.org/10.3390/ijms19103111.

(43) Awaja, F.; Zhang, S.; Tripathi, M.; Nikiforov, A.; Pugno, N. Cracks, Microcracks and Fracture in Polymer Structures: Formation, Detection, Autonomic Repair. *Progress in Materials Science* **2016**, *83*, 536–573. https://doi.org/10.1016/j.pmatsci.2016.07.007.

(44) Xu, D.; Ma, Y.; Han, X.; Chen, Y. Systematic Toxicity Evaluation of Polystyrene Nanoplastics on Mice and Molecular Mechanism Investigation about Their Internalization into Caco-2 Cells. *Journal of Hazardous Materials* **2021**, *417*, 126092. https://doi.org/10.1016/j.jhazmat.2021.126092.

(45) Llorca, M.; Farré, M. Current Insights into Potential Effects of Micro-Nanoplastics on Human Health by in-Vitro Tests. *Front. Toxicol.* **2021**, *3*. https://doi.org/10.3389/ftox.2021.752140.

(46) Mattioda, V.; Benedetti, V.; Tessarolo, C.; Oberto, F.; Favole, A.; Gallo, M.; Martelli, W.; Crescio, M. I.; Berio, E.; Masoero, L.; Benedetto, A.; Pezzolato, M.; Bozzetta, E.; Grattarola, C.; Casalone, C.; Corona, C.; Giorda, F. Pro-Inflammatory and Cytotoxic Effects of Polystyrene Microplastics on Human and Murine Intestinal Cell Lines. *Biomolecules* **2023**, *13* (1), 140. https://doi.org/10.3390/biom13010140.

(47) Lee, D.-H.; Kim, W.-H.; Lee, K.; Na, I.; Fu, X.; Jeong, H. W.; Chung, J.-O.; Roh, J.; Kim, W.; Shim, S.-M. Green Tea Extracts Rich in Epicatechins Inducing Aggregation and

View Article Online
DOI: 10.1039/D6NR00796A

Inhibiting Absorption of Amine Surface Functionalized Polystyrene Microplastics *in Vitro* Mimick System. *Journal of Hazardous Materials Advances* **2024**, *15*, 100437. https://doi.org/10.1016/j.hazadv.2024.100437.

(48) Singh, B. N.; Shankar, S.; Srivastava, R. K. Green Tea Catechin, Epigallocatechin-3-Gallate (EGCG): Mechanisms, Perspectives and Clinical Applications. *Biochemical Pharmacology* **2011**, *82* (12), 1807–1821. https://doi.org/10.1016/j.bcp.2011.07.093.

View Article Online
DOI: 10.1039/D6NR00796A

Data availability

The data supporting this article have been included as part of the Supplementary Information (SI). Supporting information: SERS detection of nanoplastics, effect of heating on SERS detection, and raw SERS spectra of NP release across different conditions (PDF). See DOI: